Fuzzy Contour Tracking of Human Silhouettes

Timothy C. Havens, *Student Member, IEEE*, Gregory L. Alexander, James M. Keller, *Fellow, IEEE*, Marjorie Skubic, *Member, IEEE*, and Marilyn Rantz

***Abstract*—Video-based tracking of contours on the human body has been shown to be useful for many applications, including gait and gesture recognition, posture estimation, and activity analysis. We present a contour tracking method that incorporates a novel edge feature and fuzzy contour template. We apply our method in tracking the motions of older adults exercising in a gym environment. The output of our system is a dynamic fuzzy representation of the spine angle of the subject. We show that the method described in this paper is capable of tracking contours even in cases where human silhouette extraction is poor.**

I. Introduction

Human motion capture is a multi-million dollar industry that continues to grow in not only the movie and video-game industries, but also in the defense and medical industries. Motion capture technology has been used to improve medical analysis of the spinal column [1], aid in MRI research and analysis [2], and analyze the movements of cyclists and snowboarders [3]. Additionally, markerless motion capture, or the measurement of motion with no explicit markers placed on the human body, has potential to both reduce the cost of motion capture (a Vicon system can cost upwards of $100,000) and to broaden the application areas.

This paper address elder care as an application area. For the purpose of measuring gait and posture information, we developed a novel algorithm to track the spine and shoulders of humans who are exercising . Our recent study, described in [4], examined how markerless motion tracking could be used to help older adults exercise more safely. This study was conducted with 38 older adult participants in a gym environment. A custom interface provided feedback to the participants about their gait and posture. Key informant interviews were conducted and phenomena that appeared across all the interviews were identified. Preliminary results are presented in [4].

The work described in this paper is a significant extension of the contour tracking method in [4]. We discovered that the system described in [4] encountered problems, including loss of track and degraded accuracy, in the presence of incomplete and noisy silhouettes (which we frequently encountered in our real-world study). The system outlined in this paper aims to improve the tracking in situations where silhouettes are not perfect.

T.C. Havens, J.M. Keller, and M. Skubic are with the Department of Electrical and Computer Engineering, University of Missouri, Columbia, MO 65211, USA (email: havenst@gmail.com, {kellerj, skubicm}@missouri.edu).

G.L. Alexander and M. Rantz are with the Sinclair School of Nursing, University of Missouri, Columbia, MO 65211, USA (email: {alexanderg, rantzm}@missouri.edu).

A novel edge feature, fuzzy template matching method, and fuzzy output system is described in Section II. Section III presents results of a simulation as well as real world results of tracking human exercise. Section IV concludes this paper.

A. Related Work

Human motion analysis is a well-researched topic pertinent to many fields, including sports medicine, nursing, physical therapy and rehabilitation, and surveillance. Special issues of journals and tracks in computer-vision conferences have been completely dedicated to human motion analysis in video.

References [5; 6] provide a good background on human motion analysis techniques. In [7], the author proposes a method to analyze human pose during exercise. The strength of this method is that it is generalizable to any pose; however, as the author points out, it is also very error-prone. An assumption that is made in [7] is that the subject is facing the camera and upright. We wish to measure the angle of the spine from the side view in both upright (treadmill) and sitting (overhead pull-down) poses; hence, the assumption in [7] makes it unsuitable for our research.

Active contours, called snakes [8], have been used to track facial features (e.g. eyebrows and mouth) and human forms in video. Although this method is effective, it is not capable of measuring the posture information we require. For instance, measuring the angle of the spine with respect to the horizontal with an active contour is not straight-forward, as active contours are not rigid, static features. However, one of the features of the contour templates in our method is the rotation angle. Hence, we use a contour tracking method based on the edge distance transform [9] with rigid, static templates.

Reference [10] describes a method which applies fuzzy logic to active contours to detect contours in MRI images and to track targets in video. This method is effective for the detection of strong contours in MRI images and for tracking human-like objects in video, but it is not easily adapted to track specific contours, as our method does.

II. Methods

The methods presented in this paper are generalizable to any problem in which contour tracking is necessary; however, we focus on tracking the contours of humans who are exercising. The two contours we are interested in are the edge of the back (spine) as seen from the side view and the shoulders as seen from the rear or front view. This paper focuses on the method, we only show results for spine tracking.

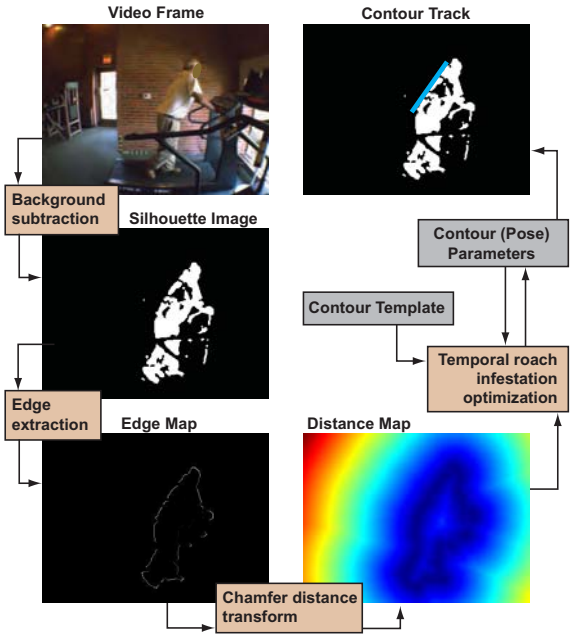

Fig. 1: Block diagram of exercise-feedback system components — spine tracking on side view of treadmill exercise.

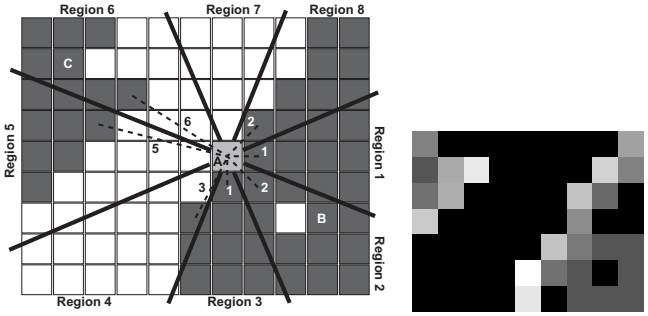

(a) Polar edge feature calculation example, $N_a = 8$ — dark pixels indicate silhouette pixels

(b) Edge map values

Fig. 2: Polar edge feature example

The environment in which we conducted this research was a public gym; hence, our ability to control experimental conditions, such as lighting conditions, background environment, and subject's clothing, was very limited. One of the problems we encountered when extracting silhouettes from the videos was incomplete or degraded silhouettes. The lighting in this environment was poor, the clothing of some participants blended in with the background, and there were occlusions present (see Figs. 1 and 4 for evidence of these problems). The silhouette shown on the middle left in Fig. 1 shows an example where the silhouette of the participant has incomplete regions in the torso and is occluded by the treadmill rails in the legs region. It is clear to the human observer where the edge of the true silhouette is in this view. However, if we used a standard edge-extraction algorithm such as a Sobel operator or first-difference calculation, the edges of the "holes" in the silhouette would have equal weight as the true exterior edges. Our contour tracking method tracks the edge of the silhouette; we created a novel edge feature with the aim of addressing the problems created by degraded silhouettes.

Figure 1 illustrates our approach in a block diagram. First, the silhouette of the human in each video frame was computed as shown in the upper left of Fig. 1. We used a statistics-based background subtraction algorithm that is adapted from [11]. Foreground pixels are denoted by $S(i, j, f) = 1$, where this is the ith row, jth column, and fth frame, and background pixels are denoted $S(i, j, f) = 0$. Second, a novel polar-distance-based edge-detection method extracts the edges of the silhouettes and gives each edge pixel a confidence value (lower left of block diagram). Third, we compute a modified chamfer distance transform of each edge map. The chamfer distance map provides an error surface upon which we can fit a contour template. The contour template scoring function includes a spatial fuzzy membership to account for uncertainty in the template shape. We also append the scoring function with a temporal damping function which penalizes candidate solutions that are significantly different from the previous frame's solution. We used *Roach Infestation Optimization* (RIO) [12] to find the best position of the contour template, which, ideally, is located on the body contour of interest, either on the back or spine. The upper right image in Fig. 1 shows the spine contour template in blue. Finally, we developed a fuzzy output that displays the angle of the spine as a temporal (or, perhaps, Type-II) fuzzy membership.

We now describe in more detail each element shown in the block diagram, Fig. 1.

A. Fuzzy Edge Feature

Our edge feature represents the confidence of each edge in the image as belonging to an exterior edge. For each pixel in the silhouette, the algorithm calculates the minimum distance to neighboring silhouette pixels in each of N_a polar regions. Figure 2(a) shows how these distances are calculated for $N_a = 8$ regions. Each of the labeled regions represents the polar slices in which a distance is calculated from the silhouette pixel labeled 'A'. In each region the L1 (or Manhattan) distance is calculated for the nearest silhouette pixel. For example, in Region 6 shown in Fig. 2(a) the nearest silhouette pixel is 8 units away, and in Region 8 the nearest pixel is 2 units away. Each silhouette pixel is thus associated with N_a distances, which we denote $\mathbf{D}(i, j, f) = \{d_1, \ldots, d_{N_a}\}$.

In the case where a nearest silhouette pixel does not exist in a region, such as Region 7, this distance is set to $(N_r + N_c)/2$, where N_r is the number of rows and N_c is the number of columns in the silhouette image. The value of the edge map for each silhouette pixel is calculated as

$$G(i, j, f) = \begin{cases} 0, & S(i, j, f) = 0; \\ \overline{\mathbf{D}}(i, j, f), & S(i, j, f) = 1, \end{cases} \quad (1)$$

where $\overline{\mathbf{D}}(i, j, f)$ is the mean value of the distance values in $\mathbf{D}(i, j, f)$. We then normalize $G(i, j, f)$ such that the

maximum value is 1. Figure 2(b) shows the values of the edge features for the silhouette pixels shown in Fig. 2(a). Note that the edge map is only shown for the interior 8×8 region of the image as this edge calculation is not valid for border pixels. Notice that the pixels around the "hole" next to pixel 'B' have a very small confidence of being edges. This is a strength of our edge detection method.

Examples of the edge map for video frames from our study are shown in Fig. 1 and Fig. 4(d). The edge map calculation gives high confidence to the exterior edges of the silhouette, while the interior edges, such as those caused by the occluding bars in the foreground and the holes in the silhouette, are virtually invisible.

B. Scoring Function

We adapt the chamfer distance transform, described in [9; 13], and define

$$C(r,c,f) = \min_{\{\forall i,\forall j: G(i,j,f)>\alpha\}} \left[(r-i)^2 + (c-j)^2\right] \quad (2)$$

Essentially, Eq.(2) calculates the minimum squared distance between each pixel location and the nearest edge map pixel greater than α. The parameter α allows the user to throw out edge map pixels that are below the value α or, in essence, unimportant edges. In this paper, we use the value $\alpha = 0.1$. We compute Eq.(2) for each pixel in the image and this distance transform map can be used to determine the best location for a contour template. Let T be a template, i.e. T is a set of coordinates describing a shape. The template is a discrete list of pixel coordinates, which define the template shape. For example, a linear (line) template, such as that used to track the spine, could be defined as

$$\mathbf{T} = \{[0\ 0]^T, [0\ 1]^T, [0\ 2]^T\},$$

where, in this example, $\mathbf{T}$ is a vertical line, three pixels long. This template formulation is very general and can represent any types of shapes, including lines, curves, and broken shapes. For a given set of template parameters, where x_f and y_f are the translations and θ_f is the rotation, the template error score is

$$M(\vec{x}_f, f) = \sum_{\{(r,c)\in T\}} 1/(1 + C(r,c,f)), \quad (3)$$

where $\vec{x}_f = (x_f, y_f, \theta_f)$. Essentially, for a given translation and rotation of the template, Eq.(3) sums up the reciprocal of the pixels in $C(r,c,f)$ that are underneath the template.

However, consider that there is an associated uncertainty to the template shape in the form of a two-dimensional (2D) fuzzy membership $\mu_T(i,j)$. This membership represents the uncertainty of the template in matching the desired contour on the silhouette image. In this paper we use a circularly symmetric triangle function in the form

$$\mu_T(i,j) = \begin{cases} 0, & \sqrt{i^2+j^2} > R; \\ 1 - \sqrt{i^2+j^2}/R, & \sqrt{i^2+j^2} \le R. \end{cases} \quad (4)$$

The value R determines the degree of uncertainty of the membership function, where small values of R create a narrow uncertainty region and large values of R create a broad uncertainty region.

We incorporate $\mu_T(i,j)$ into the template score $M(\vec{x}_f, f)$ by taking the maximum value of the membership product with the edge map at each template location (as defined by the translation and rotation parameters). The fuzzy template score is

$$M_\mu(\vec{x}_f, f) = \frac{1}{N_T} \sum_{\{(r,c)\in T\}} \bigvee_{i,j} \frac{1}{1 + C(r+i, c+j, f)} \mu_T(i,j), \quad (5)$$

where N_T is the number of pixels in the template. This normalization factor ensures that $M_\mu \in [0,1]$.

Given Eq.(5), the best contour template location solves the minimization

$$\vec{x}_{\text{best},f} = \arg\min_{\vec{x}_f} \left(1 - M_\mu(\vec{x}_f, f)\right). \quad (6)$$

We used a straight line to model the contour of the spine. The size of the templates were customized for each participant. If one wished to use our technique to track other body contours, a template could easily be designed. Eq.(5) is a score of the fit of the contour template, for a given parameter vector $\vec{x}_f$, to the edge of the silhouette in frame f. The coordinates (r,c) over which the summation in Eq.(5) is computed are found by the linear transformation

$$\begin{bmatrix} c \\ r \end{bmatrix}_i = \begin{bmatrix} \cos\theta_f & -\sin\theta_f \\ \sin\theta_f & \cos\theta_f \end{bmatrix} [\mathbf{T}_i] + \begin{bmatrix} x_f \\ y_f \end{bmatrix}, \quad (7)$$

where $[\mathbf{T}_i] = [t_c\ t_r]_i^T$ is the coordinates of the ith pixel in the contour template $\mathbf{T}$. Our algorithm defines the center of the template as the origin, but this is arbitrary.

C. Temporal Contour Search

Under ideal circumstances where a "good" silhouette image can be computed, solving Eq.(6) with an optimization method would be sufficient to track the contours. However, we conducted this research in a gym-environment; hence, "good" silhouettes were not always achieved. We added a temporal term to Eq.(6) that limited the candidate contour locations $\vec{x}_f$ to those that only changed slightly from the previous frame. In other words, because we tracked human motion, we assumed that the contours only moved a small amount between video frames (video was taken at 7.5 frames-per-second). For each video frame, the error function that must be minimized is the fuzzy union of the complement of M_μ and a temporal damping function P. The temporal template scoring function is

$$E(\vec{x}_f, \vec{x}^*_{f-1}, f) = \max\{P(\theta_f, \theta^*_{f-1}), (1 - M_\mu(\vec{x}_f, f))\} \quad (8)$$

where θ^*_{f-1} is the previous frame's best rotation parameter solution and $P(\theta_f, \theta^*_{f-1})$ is the membership in "rotated more than expected for one video frame". The temporal damping function was designed such that large changes in the template parameters produced high membership. We used

the following formulation for the membership P

$$P(\theta_f, \theta^*_{f-1}) = \begin{cases} 0, & \bar{\theta} \leq a \\ 2\left(\frac{\bar{\theta}-a}{b-a}\right)^2, & a \leq \bar{\theta} \leq \frac{a+b}{2} \\ 1-2\left(b-\frac{\bar{\theta}}{b-a}\right)^2, & \frac{a+b}{2} \leq \bar{\theta} \leq b \\ 1, & b \leq \bar{\theta} \end{cases}, \tag{9}$$

where $\bar{\theta} = |\theta_f - \theta^*_{f-1}|$ and, a and b set the inflection points of the spline. In essence, a sets the maximum expected change in rotation between frames, while b sets the point at which candidate solutions are severely punished. Values that we found effective for our study were $a = 5$ degrees and $b = 10$ degrees. P dominates the value of E in Eq.(8) for changes in rotation angle greater than a. E reduces to M_μ for $\bar{\theta} \leq a$.

RIO [12] is an optimization method we previously developed that is based on the social behavior of cockroaches. We used RIO to optimize E for each video frame in the following way:

1) The roaches are initialized randomly within a predefined bounding box around the contour of interest — the spine or the shoulders — and within a predefined parameter space;
2) The RIO algorithm searches for the best set of parameters $\vec{x}_f$ that minimize E;
3) Advance the video frame and return to step 1.

D. Fuzzy Output

We used our method to measure the spine and shoulder angles of older adults who were exercising. Hence, the output in which we were interested was the parameters of the contour template $\vec{x}_f$ that minimized Eq.(8). Specifically, we were interested in θ_f, the rotation angle of the template. This rotation angle indicates the posture and movement of the older adult during exercise [4].

By minimizing Eq.(8) a crisp output is returned from the system; namely, a horizontal and vertical translation and a rotation angle. We also developed a method which returns the output of the system as a fuzzy membership function. Consider that the parameters $\vec{x}'_f = \{x'_f, y'_f, \theta'_f\}$ minimize Eq.(8) for a given silhouette frame f. The spine angle membership function is thus computed as

$$\mu_{\text{angle}}(\theta, \vec{x}'_f, \vec{y}'_f) = \frac{1}{N_T} \sum_{\{(r,c)\in T|\{x'_f, y'_f, \theta\}\}} \bigvee_{i,j} G(r+i, c+j, f) \cdot \mu_T(i,j), \tag{10}$$

where, recall, G is the edge map and $\mu_T(i,j)$ is the template spatial uncertainty membership. Notice that this equation is virtually identical to Eq.(5), except that the chamfer distance is replaced by the edge map. Essentially, this membership function computes the fuzzy score of the match of the contour template and the edge map for a given template rotation θ. Note that $\mu_{\text{angle}}(\theta) = 1$ if and only if the contour template perfectly matches the edge map for a given rotation angle θ and $\mu_{\text{angle}}(\theta) = 0$ if and only if the edge map is zero-valued for every pixel in the computation of Eq.(10).

For a given silhouette frame f, we compute the output membership given by Eq.(10) for a discrete set of angles. This membership function can be though of as either a dynamic fuzzy membership or as a Type-II membership. For example, one could imagine that the memberships could be aggregated across frames into a Type-II membership, where the *field-of-uncertainty* represents the movement of the human and the Type-I membership is the uncertainty in the measurement.

In Example 1, we compute the output membership for $\theta = \{-50, -48, -46, \ldots, 46, 48, 50\}$ degrees, where $\theta = 0$ degrees is vertical for the spine tracking method. We then display the membership at each frame f as the fth column of an image. The following example shows the strength of showing the output as a fuzzy membership.

Example 1. We used out method to track a silhouette represented by a 70-pixel length line in an image, shown in Fig. 3(a), and a similarly sized curve in an image, shown in Fig. 3(b). The contour template was an exact match to the line; hence, this scenario is an ideal case for tracking the line. We then used our method to track each silhouette as the shape was rotated between each frame with an angle shown in Fig. 3(c), where 0 degrees indicates vertical and the views shown in Figs. 3(a,b) are vertical.

Figure 3(d) shows the resulting output membership for the line silhouette tracking example. Notice that the membership at each frame is sharply peaked at the correct rotation angle, which is what is expected for this ideal scenario.

Figure 3(e) shows the resulting output membership for the curve silhouette tracking example. Compare the output membership of the curve silhouette tracking to the line tracking. The curve output membership is much more spread out across the angles with the high (red) membership values spread out over approximately 10 degrees, compared to 2-4 degrees for the line silhouette. Additionally, the maximum membership for the curve example is approximately 0.4, compared to 0.8 for the line example.

This example shows the strength in displaying the angle output as a fuzzy membership, as opposed to a crisp output. While the overall rotation movement of both the line and curve silhouettes is easily discerned from the images, these images also show the overall confidence in the measurement.

III. Results

Example 2 illustrates the effectiveness of our proposed approach for a case of poor silhouette quality. This example tracks the spine of a study participant while they exercise on the treadmill. Video was captured at 7.5 frames per second with a standard 640×480 web cam. The length of the spine contour template in this example is 70 pixels for both the crisp method [4] and the proposed method. Each algorithm was run with the same temporal damping parameters and initialization.

Example 2. This example shows the strength of our method in measuring the motion of a human walking on the treadmill

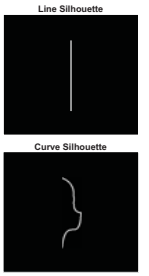

(a) Silhouettes

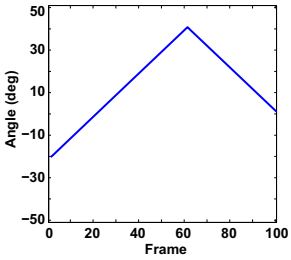

(b) Rotation angle of silhouette

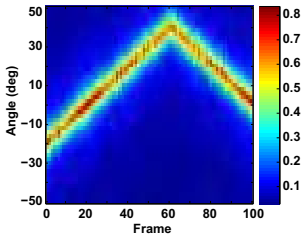

(c) Fuzzy angle output membership for line silhouette

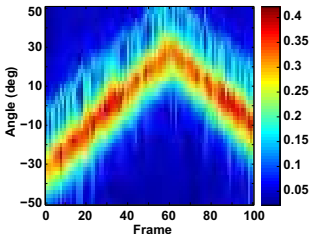

(d) Fuzzy angle output membership for curve silhouette

Fig. 3: Example of fuzzy angle output memberships for line silhouette and curve silhouette. Membership outputs are normalized to show the most color resolution in the output.

(a) Side view of treadmill exercise

(b) Silhouette

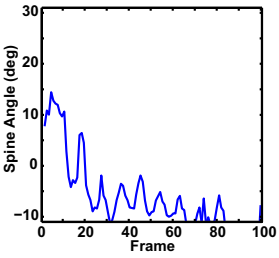

(c) Crisp spine angle as computed by method in [4]

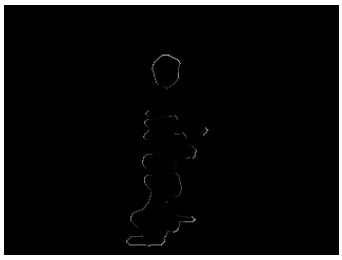

(d) Fuzzy edge map

Fig. 4: Comparison of crisp contour tracking method and proposed method for a treadmill exercise video with poor silhouette extraction.

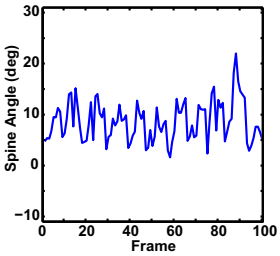

(a) Contour template rotation angle θ'_f

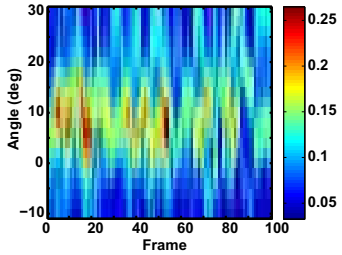

(b) Fuzzy angle output membership

Fig. 5: Contour template rotation angle θ'_f versus frame f and fuzzy angle output membership for treadmill video in Example 2.

when the video is of poor quality. Figure 4(a) shows one video frame. The video is severely saturated around the participant's torso because of sun from the windows on the right side of the image. This saturation causes problems in the silhouette extraction, which is shown in Fig. 4(b). The silhouette in the torso is broken up, with large gaps around the shoulders and waist. This problem was compounded by the white shirt that the participant was wearing, which blended with the saturated background.

We used our crisp contour tracking method, described in [4], to track the spine angle of the participant as they walked on the treadmill. Figure 4(c) is the plot of the spine angle versus frame number. This plot shows that the participant's spine angle begins at about 10 degrees. Following the first few frames, the crisp tracking method loses track and starts tracking interior edge pixels in the silhouette (see Fig. 6). Visual inspection of the video demonstrates that this measurement is not accurate. We estimate that the participant's spine angle stayed around 10 degrees, with a little variation from normal walking movement. The crisp method is flawed because it treats the edges within the "holes" in the silhouette as equal to the exterior edges. For comparison, Fig. 4(d) is an image of the fuzzy edge map. The interior edges are given a low confidence value, which, we show later, helps in tracking the spine region of the broken up silhouette.

Figure 5 shows the spine angle returned by the proposed method in view (a) and the fuzzy angle output membership in view (b). The measured rotation angle oscillates around 10 degrees as opposed to the crisp method, shown in Fig. 4(c), which does not maintain a consistent track. Also, as seen in the fuzzy output in Fig. 5(b), the high membership values all occur around 5-10 degrees. The overall membership is low, with a peak at approximately 0.25. This low membership shows that the confidence in the measurement is low. This is expected and is because of the poor silhouette.

Finally, Fig. 6 shows tracking sequences of the crisp tracking method and the proposed method. The tracking sequence of the crisp method shows that the contour template is not tracking the exterior of the spine region and is, instead, tracking edges that are internal to the silhouette. In contrast, the proposed method accurately tracks the exterior of the spine region.

IV. Conclusions and Future Work

Our qualitative study, described in [14] and [4], showed that markerless motion capture technologies can be used to assist older adults as they exercise. The study participants were interested in seeing their images with the contour tracking information and found that the processed images helped them determine whether they were interacting with

(a) Crisp method — spine tracking

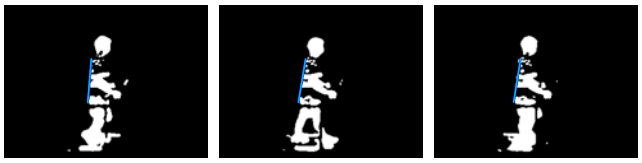

(b) Proposed method — spine tracking

Fig. 6: Comparison of spine tracking on poor silhouettes with the crisp method [4] and the proposed method — frames $\{1, 6, 11\}$ shown.

the exercise equipment (treadmill, overhead lateral pull-down, and bicycle) properly.

Additionally, many participants expressed fear of losing their balance and falling while walking; they indicated that the images provided them the ability to see whether they were maintaining good balance over the core of their body, which is important to prevent falls. Some participants indicated the images would provide added value to their exercise, making them feel safer, less likely to be injured, and less likely to fall. Others participants indicated that the images were useful but could not really take the place of a trainer in helping them reach their exercise goals.

The markerless system has potential uses for the clinician as well. Quantitative information can be derived from the kinematic data to use as baseline measurements for comparisons throughout a rehabilitation program. Periodic feedback using the system could be used to track progress and help with patient education regarding body mechanics that prevent further postural abnormalities and consequent adaptations.

The clinician will be able to collect objective data concerning posture during different functional activities and assess symmetry of movement between left and right sides. Immediate postural feedback is available to the patient and the therapist to facilitate correction of faulty positions and movements during exercise. The ability to look at specific contours on the video will help emphasize potential problem areas specific to the patient.

In conclusion, the contour tracking method we present in this paper has direct and pertinent benefits. We validated our method against a gold-standard motion capture system, the Vicon 3D marker-based system, and showed that our system is accurate in measuring the angle of the spine and shoulders relative to the horizontal floor plane.

In the future we will adapt the contour tracking methods for use in home environments. A large part of our ongoing eldercare research focuses on the use of technology to help older adults maintain independence. We are investigating the use of anonymous silhouette-based techniques to detect falls, assess mobility, and perform activity analysis. These techniques are important to effectively and inexpensively address the needs of our growing aged population.

Acknowledgment

This work was supported by the RAND/Hartford Foundation, (Award #: 9920070003), by the National Science Foundation, (Award #: IIS-0428420), and the Agency for Healthcare Research and Quality, (Award #: K08HS016862).

References

[1] G. Balint, Z. Dezso, A. Hunka, J. Lenti, and I. Lovanyi, "Motion capture vs traditional medical examinations," in *Proc. SETIT*, Tunisia, March 2005.

[2] L. Yahia-Cherif, B. Gilles, T. Molet, and N. Magnenat-Thalmann, "Motion capture and visualization of the hip joint with dynamic MRI and optical systems," *Computer Animation and Virtual Worlds*, vol. 15, no. 3-4, pp. 377–385, July 2004.

[3] B. Rosenhahn et al., "Markerless motion capture of man-machine interaction," in *Proc. CVPR*, Anchorage, AK, June 2008.

[4] T. Havens, G. Alexander, C. Abbott, J. Keller, M. Skubic, and M. Rantz, "Contour tracking of human exercises," in *Proc. IEEE CIVI*, Nashville, TN, March 2009.

[5] L. Wang, W. Hu, and T. Tan, "Recent developments in human motion analysis," *Pattern Recognition*, vol. 36, no. 3, pp. 586–601, March 2003.

[6] S. Mubarak, "Understanding human behavior from motion imagery," *Machine Vision and Applications*, vol. 14, no. 4, pp. 210–214, September 2003.

[7] F. Zijlstra, "Silhouette-based human pose analysis for feedback during physical exercises," in *6th Twente Student Conf. on IT*, Netherlands, February 2007.

[8] M. Pardas and E. Sayrol, "A new approach to tracking with active contours," in *Int. Conf. Image Proc.*, vol. 2, Vancouver, BC, September 2000, pp. 259–262.

[9] A. Thayananthan, P. Torr, and R. Cipolla, "Likelihood models for template matching," in *British Machine Vision Conference*, 2004, pp. 949–958.

[10] W. Abd-Almageed, A. El-Osery, and C. Smith, "A fuzzy-statistical contour model for MRI segmentation and target tracking," in *Proc. SPIE*, Orlando, FL, April 2004.

[11] P. Wildenauer, A. Blauensteiner, and M. Kampel, "Motion detection using an improved colour model," *Advances in Visual Computing*, pp. 607–616, 2006.

[12] T. Havens, C. Spain, N. Salmon, and J. Keller, "Roach infestation optimization," in *Proc. SIS*, St. Louis, MO, September 2008.

[13] A. Rosenfeld and J. Pfaltz, "Distance functions on digital pictures," *Pattern Recognition*, vol. 1, no. 1, pp. 33–61, 1968.

[14] G. Alexander, T. Havens, M. Skubic, M. Rantz, J. Keller, and C. Abbott, "Markerless human motion capture-based exercise feedback system to increase efficacy and safety of elder exercise routines," *Gerontechnology 2008*, vol. 7, no. 2, p. 67, May 2008.